Journal of Solid State Chemistry 182 (2009) 1533–1537

Contents lists available at ScienceDirect

Journal of Solid State Chemistry

journal homepage: www.elsevier.com/locate/jssc

Oxygen nonstoichiometry and chemical stability of $Nd_{2-x}Sr_xNiO_{4+\delta}$

Takashi Nakamura *, Keiji Yashiro, Kazuhisa Sato, Junichiro Mizusaki

Institute of Multidisciplinary Research for Advanced Materials, Tohoku University, 2-1-1, Katahira, Aoba-Ku, Sendai 980-8577, Japan

ARTICLE INFO

Article history:
Received 5 February 2009
Received in revised form
23 March 2009
Accepted 29 March 2009
Available online 8 April 2009

Keywords:
Nd_2NiO_4
Neodymium nickelate
Layered perovskite
K_2NiF_4 type oxides
Oxygen nonstoichiometry

ABSTRACT

Nonstoichiometric variation of oxygen content in $Nd_{2-x}Sr_xNiO_{4+\delta}$ ($x = 0$, 0.2, 0.4) and decomposition $P(O_2)$ were determined by means of high temperature gravimetry and coulometric titration. The measurements were carried out in the temperature range from 873 to 1173 K and the $P(O_2)$ range from 10^{-20} to 1 bar. $Nd_{2-x}Sr_xNiO_{4+\delta}$ shows the oxygen excess and the oxygen deficient composition depending on $P(O_2)$, temperature, and the Sr content. To evaluate the characteristics of oxygen nonstoichiometric behavior, partial molar enthalpy of oxygen was calculated. The value of partial molar enthalpy of oxygen slightly approaches zero as δ increases in the oxygen excess region while that is independent of δ in the oxygen deficient region. Discussion was made by comparing data of this study with nonstoichiometric and thermodynamic data of $La_{2-x}Sr_xNiO_{4+\delta}$: $Nd_{2-x}Sr_xNiO_{4+\delta}$ show more oxygen excess than $La_{2-x}Sr_xNiO_{4+\delta}$ in the higher $P(O_2)$ region, while the nonstoichiometric behavior in the oxygen deficient composition is almost the same. The variation of partial molar enthalpy of oxygen with δ for $Nd_{2-x}Sr_xNiO_{4+\delta}$ in the oxygen excess region is much smaller than that of $La_{2-x}Sr_xNiO_{4+\delta}$. The oxygen nonstoichiometric behavior of $Nd_{2-x}Sr_xNiO_{4+\delta}$ is more ideal-solution-like than that of $La_{2-x}Sr_xNiO_{4+\delta}$.

1. Introduction

Recently, Ni based K_2NiF_4 type oxides are gathering attention in the electrochemical applications such as solid oxide fuel cells (SOFCs) [1–4], oxygen permeation membranes [4,5], and catalysts [6,7]. Among K_2NiF_4 type oxides, $Nd_2NiO_{4+\delta}$ shows excellent electrochemical properties. Porous K_2NiF_4 type oxide cathode for SOFCs shows comparable performance to the conventional perovskite based cathodes [1,2]. $Nd_{1.95}NiO_4$ electrode shows much higher performance than La_2NiO_4 electrode [2]. Additionally, $Nd_2NiO_{4+\delta}$ series oxides show higher oxygen diffusivity and surface reaction rate than $La_2NiO_{4+\delta}$ series oxides [4]. The difference of electrochemical properties may be caused by the difference of defect structure. Generally, electrochemical properties are strongly affected by the concentration of defect species. K_2NiF_4 type oxides show large oxygen excess composition [4,8–10]. This excess oxygen provides high oxygen diffusivity. Jorgensen et al. carried out the neutron diffraction measurement, and elucidated that the interstitial oxygen exists at the center of La tetrahedron in $La_2NiO_{4+\delta}$ [11]. Since the interstitial oxygen easily migrates through the *ab* plane, K_2NiF_4 type oxides show anisotropic oxygen transport properties [12]. Interstitial oxygen formation reaction is expressed by

$$\frac{1}{2}O_2 + V_i^{\times} \leftrightarrow O_i'' + 2h^{\bullet} \quad (1)$$

Here, defect species are represented by the Kröger–Vink notation [13]. Holes are subsequently created by the interstitial oxygen formation to maintain the charge neutrality. Then, the amount of interstitial oxygen can significantly affect both ionic and electronic conductivity of K_2NiF_4 type oxides. Oxygen nonstoichiometry may be the decisive factor for the electrochemical properties. For the appropriate design of the practical applications, it is essential to elucidate how oxygen nonstoichiometry emerges depending on the composition, temperature, and the atmospheric condition. However, oxygen nonstoichiometry of $Nd_2NiO_{4+\delta}$ series oxides is not yet clarified so far.

The aim of this study is to measure the oxygen nonstoichiometry of $Nd_{2-x}Sr_xNiO_{4+\delta}$ and compare it with oxygen nonstoichiometry of $La_2NiO_{4+\delta}$ series oxides. For the aim, we prepare $Nd_{2-x}Sr_xNiO_{4+\delta}$ ($x = 0$, 0.2, 0.4) and measure the variation of oxygen content by combining high temperature gravimetry and coulometric titration. Obtained data is compared with authors' previous works regarding the oxygen nonstoichiometry of $La_{2-x}Sr_xNiO_{4+\delta}$ [14]. The difference of defect structure in $Nd_{2-x}Sr_xNiO_{4+\delta}$ and $La_{2-x}Sr_xNiO_{4+\delta}$ is elucidated by the comparison.

2. Experimental

2.1. Sample preparation

$Nd_{2-x}Sr_xNiO_{4+\delta}$ ($x = 0$, 0.2, 0.4) were synthesized by a citric acid method. $Ni(NO_3)_2 \cdot 6H_2O$ (99.95%, KANTO CHEMICAL) was

* Corresponding author. Fax: +81 22 217 5343.
E-mail address: t-naka@mail.tagen.tohoku.ac.jp (T. Nakamura).

0022-4596/$ - see front matter © 2009 Elsevier Inc. All rights reserved.
doi:10.1016/j.jssc.2009.03.021

dissolved into de-ionized water, and Nd_2O_3 (99.95%, KANTO CHEMICAL) and $SrCO_3$ (99.99%, RARE METALLIC) were dissolved into regent-grade nitric acid separately. The concentration of each solution was determined by chelate titration. These solutions were mixed together in proper ratios. An excess amount of citric acid was added to the mixed solution. A precursor was obtained by heating the solution at 573 K to remove water and nitric oxides. They were fired in air at 1273 K for 10 h. After grinding with ethanol, they were sintered again at 1473 K for 10 h. No peak of secondary phase was observed by XRD.

2.2. High temperature gravimetry

Oxygen nonstoichiometry was measured by high temperature gravimetry using electronic microbalances (Cahn D200 and Sartorius M25DP) under oxygen partial pressure from 1 to 10^{-4} bar. About 1 g of powder sample was lightly pressed into cylindrical form and heated at 1173 K to prepare porous specimen. The specimen was placed in a silica basket suspended by Pt wires from the beam of the micro balance. The oxygen partial pressure was controlled by the introduction of O_2–Ar gas-mixtures into the sample chamber, where a zirconia concentration cell was equipped to monitor the oxygen partial pressure. The equilibrium between the sample and surrounding gas phase was confirmed when both the oxygen partial pressure and the weight of the sample reached constant value. The change in oxygen content was determined from the variation of the weight, Δw_s,

$$\Delta\delta = \frac{M_s}{M_O}\frac{\Delta w_s}{w_s} \tag{2}$$

where $\Delta\delta$, M_s, M_O, and w_s are the variation of oxygen nonstoichiometry, the formula weight of the sample and oxygen atom, and the weight of the specimen, respectively. The experimental error due to the buoyancy is negligibly small compared to the weight variation due to the incorporation/release of oxygen.

The absolute value of the oxygen content was determined from the weight change of the specimen by the decomposition in H_2 atmosphere. It is confirmed by XRD measurement that the sample was decomposed to neodymium oxide, strontium oxide, and Ni, which is expressed by

$$Nd_{2-x}Sr_xNiO_{4+\delta} \rightarrow \frac{2-x}{2}Nd_2O_3 + xSrO + Ni + \frac{2+2\delta+x}{2}O \tag{3}$$

One mole of the sample will release $(2+2\delta+x)/2$ mole of oxygen. Weight loss measurements during the reduction of the sample were applied to determine the oxygen content of the specimen by the preceding researchers too [8–10].

2.3. Coulometric titration

For the conditions with the oxygen partial pressure below 10^{-3} bar, the oxygen nonstoichiometry was measured by the coulometric titration. An yttria stabilized zirconia (YSZ) tube was used as an electrolyte for a galvanic cell. Platinum paste was painted on the outside of the YSZ tube, and sintered at 1173 K for 3 h. About 0.5 g of lumps was placed into the tube and mechanically pressed so that specimen was in close contact with the tube wall. A Pt mesh was attached to specimen as an electrode. Inside of the tube was evacuated down to about 10^{-2} bar and refilled with Ar gas. The procedure was repeated a few times to reduce the residual oxygen inside the tube. Finally, the pressure of Ar gas was kept at about 1/10 bar at room temperature. The amount of oxygen which was extracted from or incorporated to the specimen was controlled by the electric charge passed through the cell. After specified amount of electric charge was passed, the electromotive force was measured to determine the equilibrium oxygen partial pressure in the tube. Under the condition that the amount of oxygen inside the tube was negligibly small, the oxygen which migrated between the specimen and gas phase was small enough to be neglected. Then $\Delta\delta$, was calculated by the equation

$$\Delta\delta = \frac{C}{2FM_s} \tag{4}$$

where C and F is the total amount of electric charge and Faraday constant, respectively. It is worth noting that data points near the plateau of δ vs. $\log P(O_2)$ region contain larger uncertainty than other data points, because equilibrium potential varies easily by the small variation of the oxygen content near the plateau region.

3. Results and discussion

3.1. Oxygen nonstoichiometry and decomposition $P(O_2)$ of $Nd_{2-x}Sr_xNiO_{4+\delta}$

Figs. 1–3 show measured oxygen nonstoichiometry of $Nd_{2-x}Sr_xNiO_{4+\delta}$ with $x = 0$, 0.2, and 0.4, respectively. In the figures, closed symbols show the data points measured by high temperature gravimetry, and open symbols show those measured by the coulometric titration. It is confirmed that the results of the coulometric titration and high temperature gravimetry show no discrepancy. The combination of the coulometric titration and high temperature gravimetry measurements provides useful oxygen nonstoichiometric information as reported in earlier works such as $La_{2-x}Sr_xNiO_{4+\delta}$ [14], $La_{1-x}Sr_xMnO_{3-\delta}$ [15], and $La_{2-x}Sr_xCuO_{4-\delta}$ [16]. The plateau of δ vs. $\log P(O_2)$ curve is observed near the stoichiometric oxygen content for all the composition studied. According to Wagner, the slope of δ vs. $\log P(O_2)$ curve for oxygen nonstoichiometric compounds shows minimum value at the stoichiometric composition [17]. Our results are consistent with this theory.

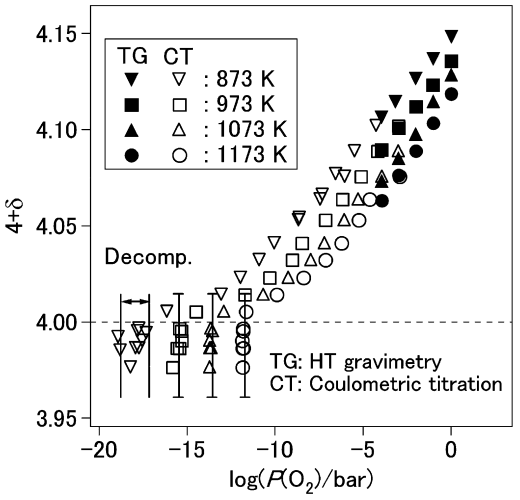

Fig. 1. Oxygen nonstoichiometry of $Nd_2NiO_{4+\delta}$. Open symbols and closed symbols were measured by coulometric titration and high temperature gravimetry, respectively.

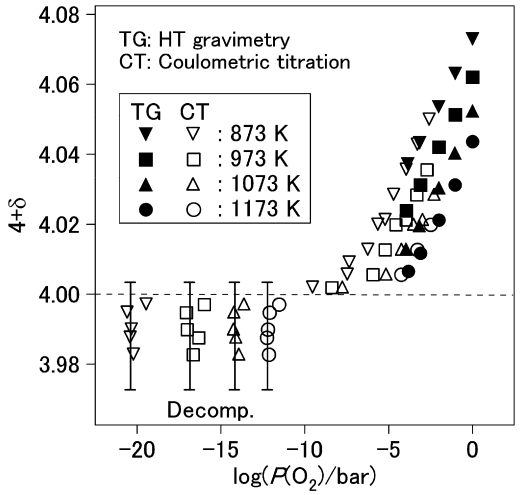

Fig. 2. Oxygen nonstoichiometry of $Nd_{1.8}Sr_{0.2}NiO_{4+\delta}$. Open symbols and closed symbols were measured by coulometric titration and high temperature gravimetry, respectively.

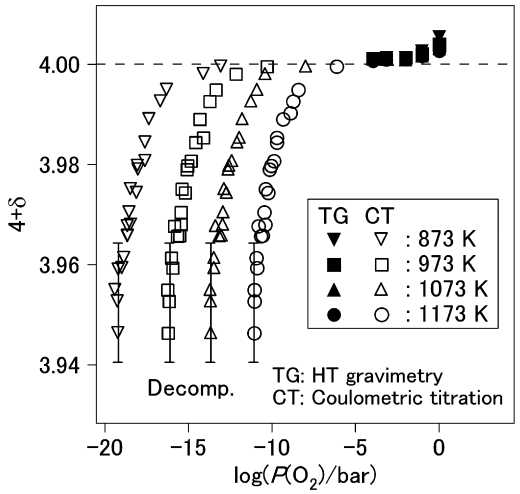

Fig. 3. Oxygen nonstoichiometry of $Nd_{1.6}Sr_{0.4}NiO_{4+\delta}$. Open symbols and closed symbols were measured by coulometric titration and high temperature gravimetry, respectively.

The range of oxygen nonstoichiometry strongly depends on the Sr content. $Nd_2NiO_{4+\delta}$ showed only the oxygen excess, while $Nd_{1.8}Sr_{0.2}NiO_{4+\delta}$ and $Nd_{1.6}Sr_{0.4}NiO_{4+\delta}$ showed both the oxygen excess in the higher $P(O_2)$ region and the oxygen deficiency in the lower $P(O_2)$ region. As the Sr content increases, the oxygen excess region decreases and the oxygen deficient region increases. As temperature increases and $P(O_2)$ decreases, the amount of the excess oxygen decreases and the amount of the oxygen deficiency increases.

The decomposition $P(O_2)$ are shown by bars in Figs. 1–3 and summarized in Fig. 4. Clear relationship between the decomposition $P(O_2)$ and the Sr content cannot be confirmed. The gap of decomposition $P(O_2)$ was observed only for $Nd_2NiO_{4+\delta}$ at 873 K. The equilibrium potential measured with elevating temperature after the oxygen extraction at 873 K is different from those measured with lowering temperature after the oxygen extraction at 1173 K. The hysteresis of oxygen nonstoichiometry near the decomposition limit was also observed in $La_2NiO_{4+\delta}$ and $LaMnO_{3-\delta}$ [14,15].

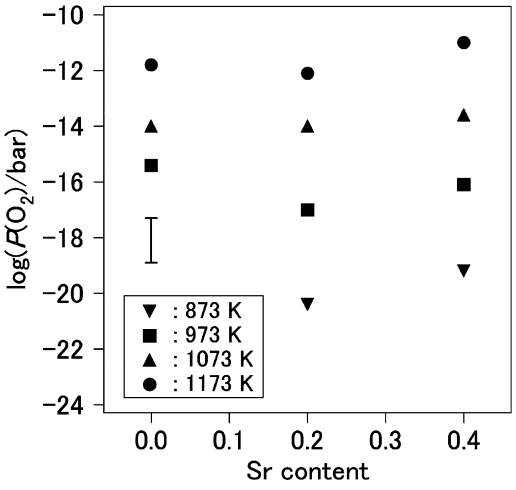

Fig. 4. Oxygen partial pressure for the decomposition of $Nd_{2-x}Sr_xNiO_{4+\delta}$.

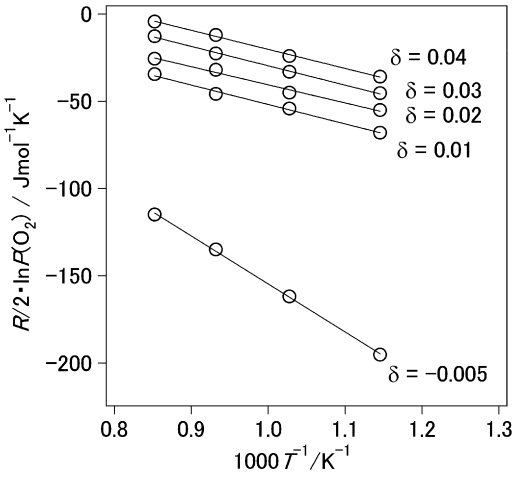

Fig. 5. $(R/2)\ln P(O_2)$ vs. $1/T$ plots of $Nd_{1.8}Sr_{0.2}NiO_{4+\delta}$.

3.2. *Partial molar enthalpy of oxygen of* $Nd_{2-x}Sr_xNiO_{4+\delta}$

Partial molar enthalpy of oxygen, $h_O - h_O^\circ$, of $Nd_{2-x}Sr_xNiO_{4+\delta}$ can be calculated by the Gibbs–Helmholtz equation by

$$h_O - h_O^\circ = \frac{\partial}{\partial(1/T)}\left(\frac{R}{2}\ln P(O_2)\right) \quad (5)$$

where R is the gas constant. Fig. 5 shows $R/2\ln P(O_2)$ vs. $1/T$ plots of $Nd_{1.8}Sr_{0.2}NiO_{4+\delta}$. From the slopes of the plots, we can obtain $h_O - h_O^\circ$ at given oxygen content. Linear relationship of the plots indicates that $h_O - h_O^\circ$ is essentially independent of temperature at the temperature range between 873 and 1173 K. Fig. 6 shows $h_O - h_O^\circ$ of $Nd_{2-x}Sr_xNiO_{4+\delta}$ as a function of δ and the Sr content. Partial molar enthalpy of oxygen show the abrupt change at the stoichiometric composition ($\delta = 0$). This abrupt change indicates that the major oxygen defect species suddenly changes at the stoichiometric composition.

Partial molar enthalpy of oxygen approaches zero slightly as δ increases in the oxygen excess region, while it is almost independent of δ in the oxygen deficient region. This means that the system behaves like an ideal solution in the oxygen deficient region, and deviates from the ideal-solution-like state in the oxygen excess region. The same tendency was observed in

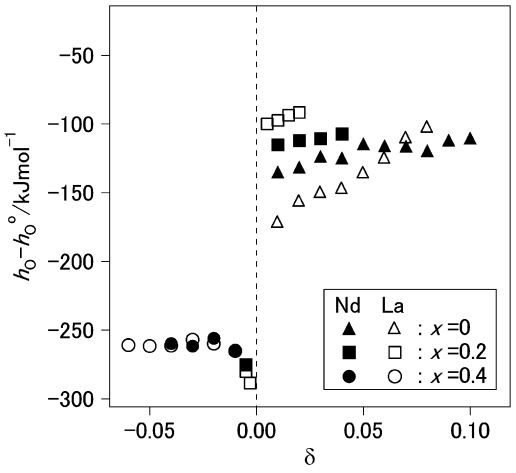

Fig. 6. Partial molar enthalpy of oxygen of $Nd_{2-x}Sr_xNiO_{4+\delta}$ (closed symbols) and $La_{2-x}Sr_xNiO_{4+\delta}$ (open symbols) [14].

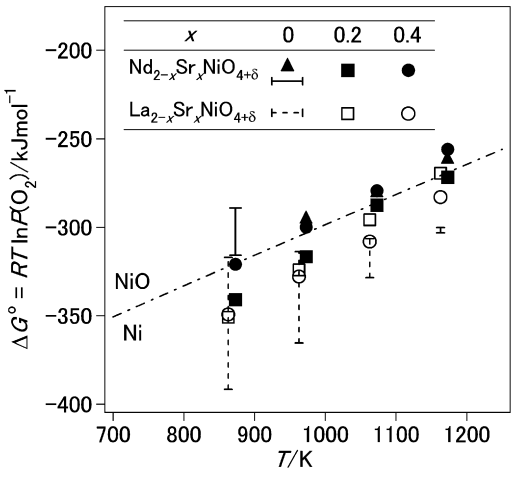

Fig. 7. Ellingham diagram of decomposition $P(O_2)$ for $Nd_{2-x}Sr_xNiO_{4+\delta}$ and $La_{2-x}Sr_xNiO_{4+\delta}$ [14]. Dashed-dotted line is decomposition $P(O_2)$ for NiO obtained by MALT [18].

$La_{2-x}Sr_xNiO_{4+\delta}$ [14]. Here, ideal-solution-like state means that the interaction among defect species is constant regardless of the defect concentration.

3.3. *The comparison of decomposition $P(O_2)$, oxygen nonstoichiometry, and partial molar enthalpy of oxygen of $Nd_{2-x}Sr_xNiO_{4+\delta}$ and $La_{2-x}Sr_xNiO_{4+\delta}$*

Fig. 7 shows the Ellingham diagram of decomposition $P(O_2)$ for $Nd_{2-x}Sr_xNiO_{4+\delta}$ and $La_{2-x}Sr_xNiO_{4+\delta}$ [14]. In both cases, decomposition $P(O_2)$ is almost independent of the Sr content. In the figure, dashed-dotted line shows the decomposition $P(O_2)$ for NiO, which is obtained from thermodynamic database MALT (Materials-oriented Little Thermodynamic database) for Windows [18]. The decomposition $P(O_2)$ for the K_2NiF_4 type oxides are similar to that of NiO at the temperature range between 873 and 1173 K. $Nd_{2-x}Sr_xNiO_{4+\delta}$ shows slightly smaller tolerance for the reduction than $La_{2-x}Sr_xNiO_{4+\delta}$. The tolerance for the reduction is essential information for the practical applications.

Fig. 8 shows the oxygen nonstoichiometry of $Nd_{2-x}Sr_xNiO_{4+\delta}$ and $La_{2-x}Sr_xNiO_{4+\delta}$ at 1073 K. As shown in the figure, $Nd_{2-x}Sr_xNiO_{4+\delta}$ shows larger oxygen excess compositions than

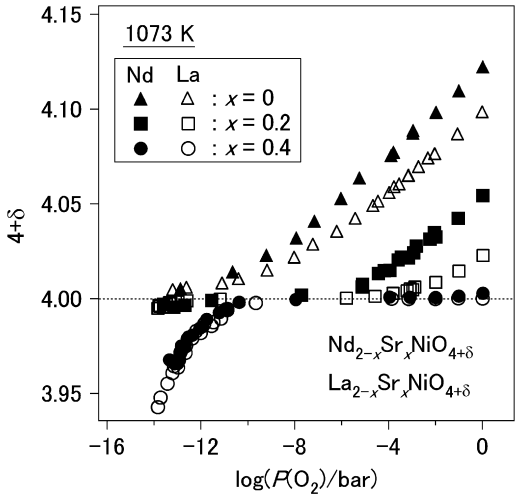

Fig. 8. Oxygen content of $Nd_{2-x}Sr_xNiO_{4+\delta}$ (closed symbols) and $La_{2-x}Sr_xNiO_{4+\delta}$ (open symbols) at 1073 K [14].

$La_{2-x}Sr_xNiO_{4+\delta}$, while the oxygen nonstoichiometric behavior of $Nd_{2-x}Sr_xNiO_{4+\delta}$ is almost the same as that of $La_{2-x}Sr_xNiO_{4+\delta}$ in the oxygen deficient region. The ionic radii of nine-coordinated La^{3+} and Nd^{3+} are 1.20 and 1.09 Å, respectively [19]. The difference of ionic radius may cause the drastic change of the oxygen nonstoichiometry in the oxygen excess region. Because the oxygen excess is caused by the interstitial oxygen and the oxygen deficiency is caused by the vacancy of oxygen sublattice in NiO_6 octahedron, Fig. 8 indicates that the space of rock salt layer is different between $Nd_{2-x}Sr_xNiO_{4+\delta}$ and $La_{2-x}Sr_xNiO_{4+\delta}$, while NiO_6 octahedron is not so different. Detail local structure information is needed for further discussion.

Partial molar enthalpy of oxygen of $La_{2-x}Sr_xNiO_{4+\delta}$ is shown in Fig. 6 as open symbols. In the oxygen excess region, the variation of $h_O - h_O^\circ$ with δ of $La_{2-x}Sr_xNiO_{4+\delta}$ is much larger than that of $Nd_{2-x}Sr_xNiO_{4+\delta}$. This means that the variation of the interaction among randomly distributed defect species of $La_{2-x}Sr_xNiO_{4+\delta}$ is more significant than that of $Nd_{2-x}Sr_xNiO_{4+\delta}$. $Nd_{2-x}Sr_xNiO_{4+\delta}$ show more ideal-solution-like nonstoichiometric behavior than $La_{2-x}Sr_xNiO_{4+\delta}$. Rosenberg suggested that the mass action law involving electronic species no longer holds in the high electron concentration systems [20]. High concentration of electronic carriers can cause the deviation of activity coefficient for electrons or holes from unity. The deviation from an ideal-solution-like state becomes more significant as electronic carrier concentration increases. Because $Nd_{2-x}Sr_xNiO_{4+\delta}$ shows larger oxygen excess than $La_{2-x}Sr_xNiO_{4+\delta}$ at given conditions, $Nd_{2-x}Sr_xNiO_{4+\delta}$ has more holes than $La_{2-x}Sr_xNiO_{4+\delta}$. If Rosenberg's theory is appropriate to K_2NiF_4 type oxides, the degree of the deviation form ideal-solution-like state will become more significant in $Nd_{2-x}Sr_xNiO_{4+\delta}$. This trend is opposite to our experimental results. Rosenberg's theory seems inappropriate to explain the oxygen nonstoichiometric behavior of K_2NiF_4 type oxides. On the other hand, Onuma et al. suggested that the departure from the ideal-solution-like state is caused by the lattice volume change induced by the defect species [21]. For K_2NiF_4 type oxides, the lattice constant change due to the composition variation along c axis is much more significant than that along a and b axes [11,22,23]. Fig. 9 shows the variation of the lattice constant along c axis with δ of $Nd_{2-x}Sr_xNiO_{4+\delta}$ and $La_{2-x}Sr_xNiO_{4+\delta}$ at room temperature [22,23]. In the figure, vertical axis shows the ratio of the lattice constant at given δ and that at stoichiometric oxygen content ($\delta = 0$). Since the data in Fig. 9 were measured at room

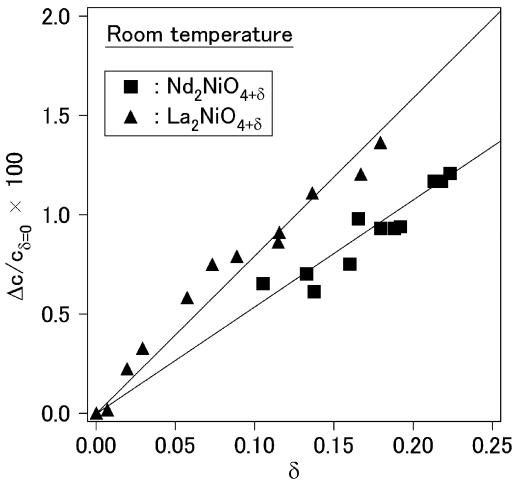

Fig. 9. The variation of lattice parameter along c axis with δ of $Nd_2NiO_{4+\delta}$ (■) and $La_2NiO_{4+\delta}$ (▲) measured at room temperature [22,23].

temperature, what we can obtain here is just a direction to elucidate the nonstoichiometric behavior of K_2NiF_4 type oxides. In both $Nd_{2-x}Sr_xNiO_{4+\delta}$ and $La_{2-x}Sr_xNiO_{4+\delta}$, crystal lattice expands along c axis as excess oxygen increases. Jorgensen et al. reported that the bond length between Ni and lattice oxygen along c axis become smaller as excess oxygen increases and the distance between Ni and lattice oxygen along a and b axes is almost independent of δ [11]. Then, the length of the perovskite layer along c axis becomes shorter as excess oxygen increases. From these reports, it is estimated that the space in the rock salt layer becomes larger as excess oxygen increases. From Fig. 9, it is confirmed that the variation of lattice constant with δ is more significant in $La_{2-x}Sr_xNiO_{4+\delta}$ than $Nd_{2-x}Sr_xNiO_{4+\delta}$. This indicates that the lattice volume change due to the excess oxygen incorporation is more significant in $La_2NiO_{4+\delta}$ than $Nd_2NiO_{4+\delta}$, i.e. $La_2NiO_{4+\delta}$ needs larger change of the lattice volume than $Nd_2NiO_{4+\delta}$ to form interstitial oxygen in the rock salt layer. From the relationship between the variation of lattice constant with δ and the variation of $h_O - h_O^\circ$ with δ, Onuma's theory seems to be appropriate to explain the nonstoichiometric behavior of K_2NiF_4 type oxides, that is, the enthalpy change due to excess oxygen is more significant in La based K_2NiF_4 type oxides than Nd based K_2NiF_4 type oxides and interstitial oxygen is formed more easily in Nd based K_2NiF_4 type oxides than in La based K_2NiF_4 type oxides. As mentioned before, this evaluation contains some uncertainty due to the mismatch of experimental conditions. However the result provides us an important clue to elucidate real defect structure in K_2NiF_4 type oxides. That is, oxygen nonstoichiometric behavior may be significantly affected by the change of crystal structure caused by the defect species. At this stage, it is difficult to elucidate the relationship between oxygen nonstoichiometric behavior and crystal structure due to the lack of structural information. For further discussion, in-situ observation of the local structure is needed.

4. Conclusions

1. $Nd_{2-x}Sr_xNiO_{4+\delta}$ shows oxygen excess and oxygen deficiency depending on temperature, $P(O_2)$, and the Sr content. As the Sr content increases, the oxygen excess region decreases and the oxygen deficient region increases. On the other hand, decomposition $P(O_2)$ of $Nd_{2-x}Sr_xNiO_{4+\delta}$ is independent of the Sr content.
2. At given conditions, the amount of excess oxygen of $Nd_{2-x}Sr_xNiO_{4+\delta}$ is larger than that of $La_{2-x}Sr_xNiO_{4+\delta}$. This may be caused by the structural difference in the rock salt layer where interstitial oxygen is located.
3. Partial molar enthalpy of oxygen, $h_O - h_O^\circ$, is calculated from experimental results with Gibbs–Helmholtz equation. Compared to $La_{2-x}Sr_x$ $NiO_{4+\delta}$, the variation of $h_O - h_O^\circ$ with δ is smaller in Nd_{2-x} $Sr_xNiO_{4+\delta}$. This means that the oxygen nonstoichiometric behavior of $Nd_{2-x}Sr_xNiO_{4+\delta}$ is more ideal-solution-like than that of $La_{2-x}Sr_x$ $NiO_{4+\delta}$.
4. Oxygen nonstoichiometric behavior of K_2NiF_4 type oxides may be significantly affected by the change of crystal structure caused by the defect species. In-situ observation of the local structure is absolutely needed.

Acknowledgments

This research was partly supported by the Grant-in-Aid for Scientific Research on Priority Area, "Nanoionics (439)" and the Grant-in-Aid for JSPS Fellowship by Ministry of Education, Science, and Culture, Sports and Technology.

References

[1] F. Mauvy, C. Lalanne, J.M. Bassat, J.C. Grenier, H. Zhao, P. Dordor, Ph. Stevens, J. Europ. Ceram. Soc. 25 (2005) 2669–2672.
[2] F. Mauvy, C. Lalanne, J.M. Bassat, J.C. Grenier, H. Zhao, L. Huo, P. Stevens, J. Electrochem. Soc. 153 (2006) A1547–A1553.
[3] A. Aguadero, J.A. Alonso, M.J. Escudero, L. Daza, Solid State Ionics 179 (2008) 393–400.
[4] E. Boehm, J.M. Bassat, P. Dordor, F. Mauvy, J.C. Grenier, P. Stevens, Solid State Ionics 176 (2005) 2717–2725.
[5] T. Ishihara, S. Miyoshi, T. Furuno, O. Sanguanruang, H. Matsumoto, Solid State Ionics 177 (2006) 3087–3091.
[6] B.S. Liu, L. Liu, C.T. Au, A.S.C. Cheung, Catal. Lett. 108 (2006) 37–44.
[7] J. Guo, H. Lou, Y. Zhu, X. Zheng, Mat. Lett. 57 (2003) 4450–4455.
[8] E.V. Tsipis, E.N. Naumovich, M.V. Patrakeev, J.C. Waerenborgh, Y.V. Pivak, P. Gaczynski, V.V. Kharton, J. Phys. Chem. Solids. 68 (2007) 1443–1455.
[9] V. Vashook, E. Girdauskaite, J. Zosel, T.L. Wen, H. Ullmann, U. Guth, Solid State Ionics 177 (2006) 1163–1171.
[10] A.V. Kovalevsky, V.V. Kharton, A.A. Yaremchenko, Y.V. Pivak, E.V. Tsipis, S.O. Yakovlev, A.A. Markov, E.N. Naumovich, J.R. Frade, J. Electroceram. 18 (2007) 205–218.
[11] J.D. Jorgensen, B. Dabrowski, S. Pei, D.R. Richards, D.G. Hinks, Phys. Rev. B 40 (1989) 2187–2199.
[12] J.M. Bassat, P. Odier, A. Villesuzanne, C. Marin, M. Pouchard, Solid State Ionics 167 (2004) 341–347.
[13] F.A. Kröger, in: The Chemistry of Imperfect Crystals vol. 2, North-Holland Publishing Company, Netherlands, 1974 (second revised edition).
[14] T. Nakamura, K. Yashiro, K. Sato, J. Mizusaki, Solid State Ionics 180 (2009) 368–376.
[15] J. Mizusaki, H. Tagawa, K. Naraya, T. Sasamoto, Solid State Ionics 49 (1991) 111–118.
[16] H. Kanai, J. Mizusaki, H. Tagawa, S. Hoshiyama, K. Hirano, K. Fujita, M. Tezuka, T. Hashimoto, J. Solid State Chem. 131 (1997) 150–159.
[17] C. Wagner, Prog. Solid State Chem. 6 (1971) 1–15.
[18] The thermodynamic database MALT for Windows; Kagaku Gijutsu Sha, 〈http://www.kagaku.com/malt〉.
[19] R.D. Shannon, C.T. Prewitt, Acta Cryst. B 25 (1969) 925–946.
[20] A.J. Rosenberg, J. Chem. Phys. 33 (1960) 665–667.
[21] S. Onuma, K. Yashiro, S. Miyoshi, A. Kaimai, H. Matsumoto, Y. Nigara, T. Kawada, J. Mizusaki, K. Kawamura, N. Sakai, H. Yokokawa, Solid State Ionics 174 (2004) 287–293.
[22] Y. Toyosumi, H. Ishikawa, K. Ishikawa, J. Alloys Comp. 408–412 (2006) 1204–1299.
[23] D.E. Rice, D.J. Buttrey, J. Solid State Chem. 105 (1993) 197–210.